

Experimental observation of two threshold fields for runaway-electron generation in the EAST tokamak

L. Zeng¹, Y. Liang², S. Lin¹, Y. Liu¹, H. Liu¹, R. Zhou¹, H. Zhao¹, A. Ti¹, Y. Jie¹, S. Zhang¹, X. Gao¹, X. Zhang¹, B. Wan¹ and the EAST team

¹Institute of Plasma Physics, Chinese Academy of Sciences, 230031 Hefei, China

²Forschungszentrum Jülich GmbH, Institute of Energy and Climate Research - Plasma Physics (IEK-4), 52425 Jülich, Germany

E-mail: zenglong@ipp.ac.cn

1. Introduction

Runaway electron (RE) currents of several mega amperes are expected to be generated in ITER disruptions via the dominated avalanche multiplication [1]. The RE seeds are mainly provided by Dreicer generation. The previous prediction shows that the threshold field for avalanche mechanism [2] is much smaller than the Dreicer generation, indicating the avalanche process appears closely after Dreicer generation. Ref. [3] demonstrates that the electric field for runaway avalanche onset is higher and the avalanche growth rate is lower than previous predictions [3]. We present here observations of two threshold fields for runaway-electron generation in the EAST tokamak.

2. Experimental observations

The experiment was done by slowly letting the density ramp down during the current flattop. EAST possesses several diagnostics able to measure the RE population, each dominantly sensitive to a different energy range: Michelson interferometer (mostly sensitive to ECE in the 0-100 keV); CdTe HXR detectors (mostly sensitive to photons in the 30-300 keV); BGO HXR detectors (mostly sensitive to photons in the 0.344-6.13 MeV) and an infrared camera measuring near-IR photons. HXR continuum emission is expected to be dominated by bremsstrahlung from fast electrons striking nuclei, while ECE and synchrotron emission is from confined electrons.

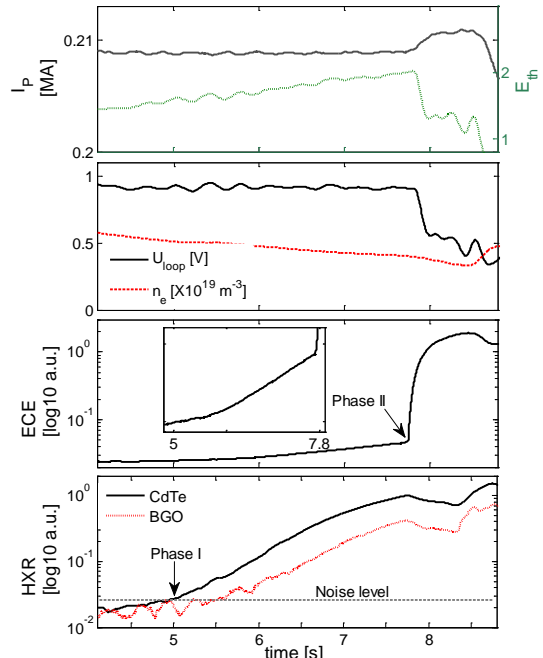


Fig. 1 Time traces in shot 53852 showing (a) plasma current and normalized electric field, (b) toroidal loop voltage and line-averaged electron density, (c) ECE signal, and (d) CdTe and BGO HXR. Dashed line indicates the noise level for CdTe and BGO detectors.

Figure 1 presents the basic plasma parameters of the ohmic discharge: the toroidal magnetic field $B_t \sim 2$ T, the plasma current $I_p \sim 0.2$ MA, the line averaged central density n_e changing from 1.0×10^{19} to 0.3×10^{19} m⁻³, and E_{th} is defined by U_{loop}/n_e . The initial density is held above 10^{19} m⁻³ which prevents slide-aways during the formation phase. After the formation phase, density is controlled to pump-out linearly, shown in Fig. 1(b). Fig. 1(d) illustrates that after some time, RE-generated HXRs become visible firstly by CdTe detectors and then by BGO detectors. The time delay is due to that low energy limit detected by BGO scintillates are higher than CdTe scintillates. Additionally, REs are also confirmed by rapid growth of ECE, contributed from fast electrons, displayed in Fig. 1(c). At the moment (~ 5 s), E-fields is about $15 \times E_{crit}$, in which $E_{crit} \approx 0.08n_{20}$.

Fig. 2(a) and (b) demonstrate the time evolution of energy spectra. The high-frequency ECE in frequency domain presents the development of a high-frequency tail concurrent with the RE growth after 5s. HXR spectra indicates RE number in the energy range from 30 keV to 250 keV continues to increase.

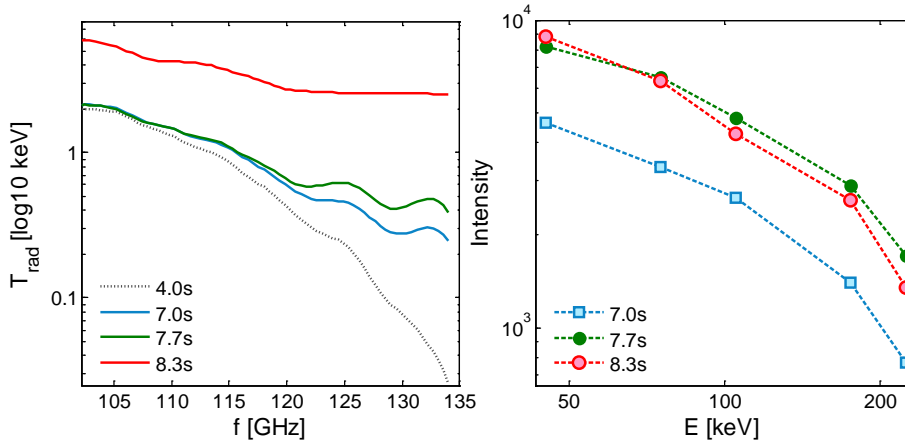


Fig. 2 (a) the ECE evolution in frequency domain and (b) the RE spectra evolution. The energy distribution is estimated from CdTe HXRs.

By continuing to ramp down the density until at E-fields that are $\approx 20 \times E_{crit}$ (~ 7.8 s), it is found that the signals of ECE grow exponentially whilst the amplitude of CdTe and BGO HXRs begin to decay. Meanwhile,

the loop voltage decreases clearly and a bump is observed in plasma current. The in frequency domain presents ECE spectra grows rapidly in a wide frequency band from 100 to 135 GHz. HXR spectra during phase II shows that the number of RE in high energy regime (>80 keV) decrease and REs in low energy regime (<80 keV) increase, showing that the RE energy spectra move to a lower energy. These results provide evidence for the occurrence of avalanche process at 7.8s. Appearance of avalanche process generates more REs and the RE current replaces part of plasma current, resulting the drop in loop voltage and the bump in the plasma current, consistent with the experimental observations.

A comparison of growth rates measures from the ECE and HXR diagnostics is shown in Fig. 3. In the phase of primary-dominated RE generation, both the ECE and HXR growth is larger than 0 and the ECE growth is quasi-linear. In the phase of secondary-dominated RE generation, the ECE signal grows exponentially but the HXR growth is less than zero, which means that the RE number in the HXR range decreases and shifts to the lower energy range, proving the onset of avalanche process.

Moreover, once the avalanche process appears, the plasma current is partially replaced by RE current and the corresponding value E_{th} also decrease clearly. Even when E_{th} is less than the critical field for Dreicer generation and the Dreicer generation is suppressed, the growth rate of ECE is still much larger than that during phase I, indicating that the avalanche process is not fully suppressed. These results suggesting that the threshold field for the onset of avalanche process is higher than the critical field to overcome the collision friction for REs and the field for the suppressing of avalanche process is still much smaller than the critical field to overcome the collision friction for REs.

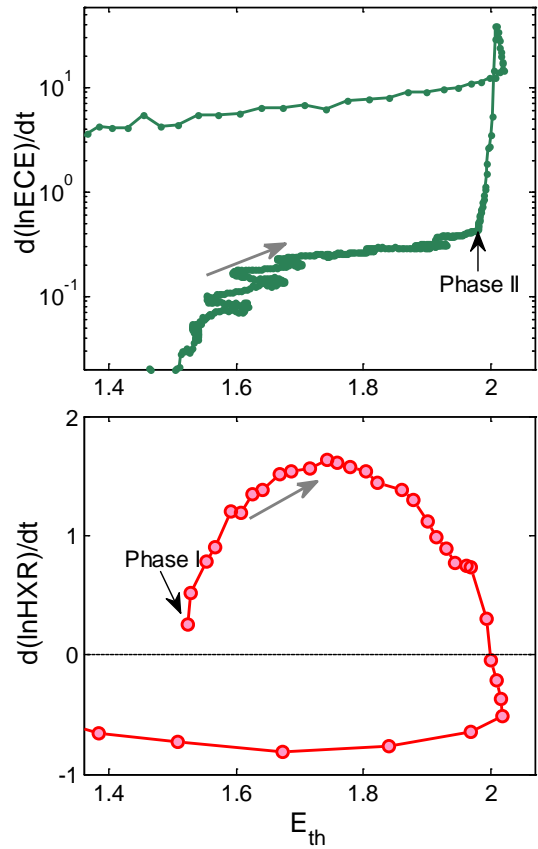


Fig. 3 Comparison of growth rates measured by ECE and CdTe HXRs. The grey arrow indicates the time evolution. The starting time of phase I and II are also labeled in the figure.

3. Discussion and conclusion

With a simple treatment of the RE generation problem, the RE growth is previously modeled as $d(n_{RE})/dt = S_{pri} + \gamma_{sec} n_{RE}$. In this model, both the Dreicer generation and avalanche process can contribute to the RE number and there is no delay between the two processes, which is not consistent with the experimental results. Based on the latest theory and the experimental results, a new 0-D RE growth model is considered as

$$d(n_{RE})/dt = S_{pri} + H(E-E_{th2}) \gamma_{sec} n_{RE}$$

Here $H(E-E_{th2})$ is the Heaviside function and E_{th2} is the threshold field for onset of avalanche mechanism.

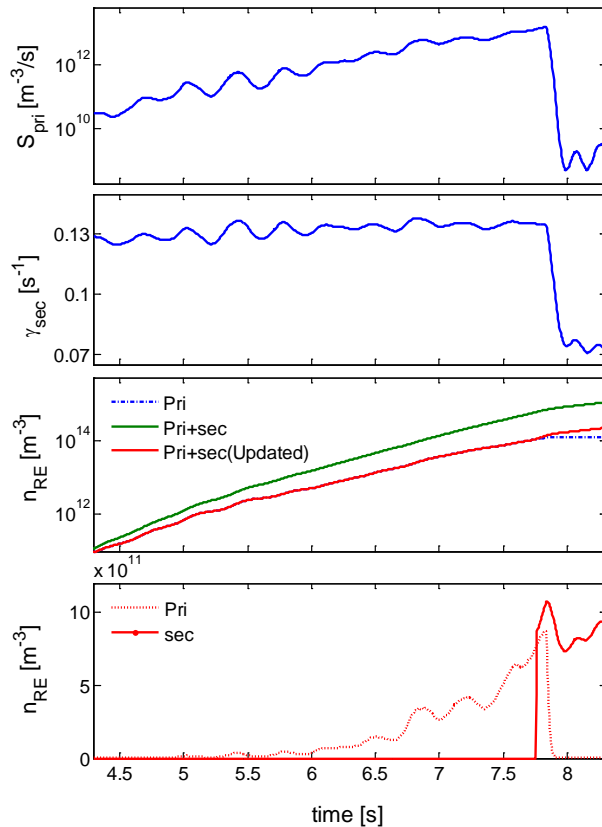


Fig. 4 Calculation of the new RE growth model.

fields (E-field), characterizing a minimal field required for sustainment of the existing runaway electron (RE) population and a higher field required for the avalanche onset [1], have been experimentally observed in the flattop of EAST discharges. These results demonstrate that the electric field for RE avalanche onset is much higher than previous predictions, which should be considered when making predictions on RE generation and mitigation in devices such as ITER and CFETR.

Acknowledgement. —Support from the National Magnetic Confinement Fusion Science Program of China under Contracts No. 2013GB106003 and 2014GB106004 and the National Natural Science Foundation of China under Contract No. 11475221 is gratefully acknowledged.

References.

- [1] T. C. Hender *et al* Nucl. Fusion **47**, S128 (2007)
- [2] M. N. Rosenbluth and S.V. Putvinski, Nucl. Fusion **37**, 1355 (1997)
- [3] P. Aleynikov and B. N. Breizman, Phys. Rev. Lett **114**, 155001 (2015)

Fig. 4 present the calculation of the new RE growth model. Fig. 4(a) and 4(b) shows the calculation results of S_{pri} and γ_{sec} . The RE density is also calculated by the previous model and the new one. In the new model, the RE density is less than the previous one, due to no contribution of the avalanche process when the electric field is less than E_{th2} , shown in Fig. 4(c). Furthermore, the calculation suggests the HXR signal can only detect $n_{\text{RE}} > O(10^{12}) \text{ m}^{-3}$. Fig. 4(d) shows that once the avalanche process appears, the contribution is as much as the Dreicer generated REs, which could explain the exponential growth of ECE and the decay of loop voltage.

Finally, two different threshold electric